Inorganic Chemistry

Communication

pubs.acs.org/IC

Intracellular Targeting and Pharmacological Activity of the Superoxide Dismutase Mimics MnTE-2-PyP^{5+} and MnTnHex-2-PyP^{5+} Regulated by Their Porphyrin Ring Substituents

Jade B. Aitken,[†] Emily L. Shearer,[‡] Niroshini M. Giles,[‡] Barry Lai,[§] Stefan Vogt,[§] Julio S. Reboucas,[∥] Ines Batinic-Haberle,[⊥] Peter A. Lay,[†] and Gregory I. Giles[‡,*]

[†]School of Chemistry, The University of Sydney, NSW 2006, Australia

[‡]Department of Pharmacology and Toxicology, University of Otago, P.O. Box 913, Dunedin, New Zealand

[§]X-ray Science Division, Argonne National Laboratory, Argonne, Illinois 60439, United States

[∥]Departamento de Quimica, Universidade Federal da Paraiba, Joao Pessoa, PB, Brazil

[⊥]Department of Radiation Oncology, Duke University, Durham, North Carolina 27710, United States

Supporting Information

ABSTRACT: Manganese porphyrin-based drugs are potent mimics of the enzyme superoxide dismutase. They exert remarkable efficacy in disease models and are entering clinical trials. Two lead compounds, MnTE-2-PyP^{5+} and MnTnHex-2-PyP^{5+}, have similar catalytic rates, but differ in their alkyl chain substituents (ethyl vs *n*-hexyl). Herein we demonstrate that these changes in ring substitution impact upon drug intracellular distribution and pharmacological mechanism, with MnTnHex-2-PyP^{5+} superior in augmenting menadione toxicity. These findings establish that both catalytic activity and intracellular distribution determine drug action.

Cellular oxidation as a result of the formation of reactive oxygen species (ROS) is observed in a wide range of diseases including cancer, dementia, cardiovascular disorders, and diabetes.[1−3] A principal ROS is the one-electron reduction product of dioxygen, superoxide. To protect against cellular damage, superoxide levels within cells are normally regulated at nM levels by the superoxide dismutase family of enzymes (SOD), which convert superoxide to hydrogen peroxide ($2O_2^{\bullet-} + 2H^+ \rightarrow H_2O_2$ and O_2). The resulting hydrogen peroxide is then scavenged by the cell's antioxidant defense network.

While superoxide is not a highly damaging ROS,[4] it is necessary to regulate its cellular concentration as it can disrupt metalloproteins. This is followed by the release of reduced metals such as Fe^{2+}, which can damage the cell via the Fenton reaction. Furthermore superoxide can act at the diffusion-limited rate with another radical, $^{\bullet}NO$, to form the potent oxidizing agent peroxynitrite ($ONOO^-$).[5] Therefore, by out-competing alternative superoxide reactions, in situ SOD can protect the cell from oxidation. This protective action of SOD is dependent upon the concentrations of all of the species involved, and a bell shaped concentration curve is often observed. As SOD levels increase they reach a protective maximum, beyond which SOD becomes a pro-oxidant due to excessive peroxide formation.[6]

Therapeutics that mimic SOD could therefore assist disease treatment, and several such drugs are approaching clinical trials. Among the most promising are Mn-containing porphyrin catalysts, of which MnTDE-2-ImP^{5+} has successfully completed a phase I clinical trial for amyotrophic lateral sclerosis.[2,3] As well as their SOD activity, these drugs also reduce other negatively charged ROS, e.g., $ONOO^-$ and $CO_3^{\bullet-}$. For the SOD reaction, the value of k_{cat} is proportional to the redox potential of the Mn center, and if this is poised around +300 mV, the drugs possess SOD activity similar to that of the native enzyme.

However, k_{cat} does not always correlate with observed in vivo activity.[2,3] Therefore, we hypothesized that additional factors that contribute to drug potency were (a) the extent of intracellular uptake or (b) the partitioning of the drugs into intracellular organelles. To investigate these cellular pharmacokinetics, synchrotron-radiation-induced X-ray emission (SRIXE) was used as a highly sensitive technique for quantitative elemental mapping.[7] SRIXE data were compared for the two structurally related Mn porphyrins, MnTE-2-PyP^{5+} and MnTnHex-2-PyP^{5+} (Figure 1).[8] These drugs have very similar

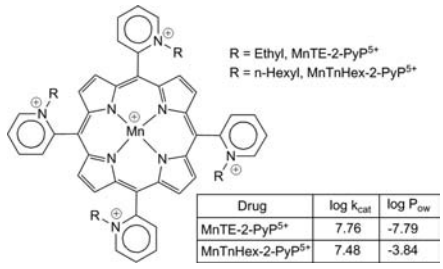

Drug	log k_{cat}	log P_{ow}
MnTE-2-PyP^{5+}	7.76	-7.79
MnTnHex-2-PyP^{5+}	7.48	-3.84

Figure 1. Structures of Mn Porphyrin-based SOD mimics.

reactivity profiles toward superoxide, $ONOO^-$ and $CO_3^{\bullet-}$[2,8,9] but differ in the length of the alkyl chain substituents (ethyl vs *n*-hexyl), possess different solubilities (log P_{OW}), and display different biological activities.

Using A549 lung carcinoma cells, the drugs were dosed over the known in vivo pharmacokinetic range (1, 10, and 100 μM)

Received: April 4, 2012
Published: April 3, 2013

   dx.doi.org/10.1021/ic300700g | *Inorg. Chem.* 2013, 52, 4121−4123

for 24 h.[10] As cultured A549 cells only contain low levels of Mn,[11] SRIXE was able to directly quantify the uptake and cellular distribution of both drugs. Analysis of the integrated fluorescence intensity demonstrated significant ($p < 0.05$) increases in the Mn signal post-drug treatment (Figure 2). These increases were

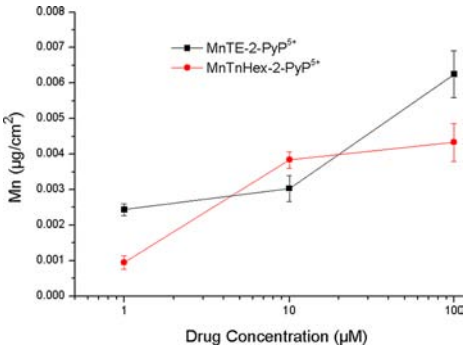

Figure 2. Cellular uptake of Mn porphyrin-based SOD mimics. Data are corrected for a background Mn level of 0.9 ng/cm^2.

dose-dependent; however, over the full concentration range the ~4-fold Mn increases inside the cell were comparatively small when compared to the 100-fold variation in the extracellular drug. At each dose, similar Mn levels were detected for both drugs (Figure 2), which indicated that, by 24 h, the large difference in solubility between the two analogues did not affect overall cellular uptake.

As A549 cells have a radius of ≈7 μm,[12] elemental densities were used to estimate cellular drug concentrations. Using 5 ng/cm^2 as the mean increase in Mn (for 100 μM drug), this corresponded to an intracellular concentration ≈ 190 μM. This remarkably high drug accumulation exceeded drug levels in the extracellular medium and explained the small increases in drug uptake over the concentration range, as intracellular levels may have approached saturation. Such a phenomenon has previously been reported for other Mn-based drugs,[13] with enhanced uptake being ascribed to the negative cell membrane potential (typically −50 mV), which drives the cellular uptake of cations.[14]

In contrast to the overall cellular concentration, analysis of the SRIXE elemental maps revealed major differences in intracellular distribution between the two analogues. For these studies the P map was used to delineate the nuclear region of the cell, due to the high concentration of P in DNA within this organelle. Comparison of the Mn to P maps indicated that, for MnTE-2-PyP^{5+}, the majority of the Mn signal directly overlapped with the nuclear region (Figure 3). However, MnTnHex-2-PyP^{5+} did not show substantial nuclear overlap, and the Mn signal was dispersed throughout the extranuclear space. Here the punctate

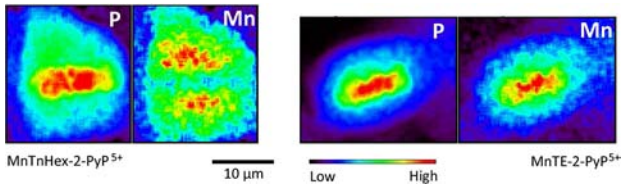

Figure 3. Representative SRIXE elemental maps of A549 cells treated with either MnTnHex-2-PyP^{5+} (left panel) or MnTE-2-PyP^{5+} (right panel) for 24 h (100 μM drug). The maps show drug localization (Mn map) in relation to the nucleus (region of highest intensity on the P map).

distribution of MnTnHex-2-PyP^{5+} may indicate its accumulation into mitochondria, which has been previously implicated in its protective mechanism.[15]

To quantify drug distribution, the nucleus and the extranuclear space were analyzed as two discrete regions, which revealed that, for a 100-μM drug addition, there was no significant difference ($p > 0.05$) in intracellular concentration (Figure 4). However, for

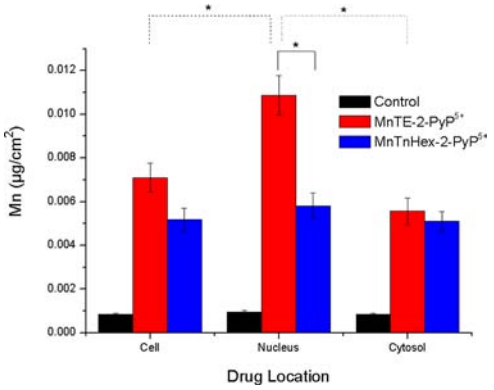

Figure 4. Quantification of drug partitioning within the cell.

MnTE-2-PyP^{5+}, the nuclear drug concentration was significantly increased 2.1-fold ($p < 0.05$), while for MnTnHex-2-PyP^{5+} levels were constant throughout the cell and the SRIXE maps indicated low nuclear localization (Figure 3). Therefore, once the drug had entered the cell, the ring substituents rather than the overall charge determined intracellular distribution. The substantial coincidence of the P and Mn maps indicated that the ethyl chain directed MnTE-2-PyP^{5+} to the nucleus, while the *n*-hexyl analogue was extranuclear and potentially associated with the mitochondria.

The molecular basis for this differential drug targeting has yet to be fully ascertained. The partitioning of a drug among intracellular organelles is dependent upon a complex array of factors including electrostatics, membrane transport, and drug binding interactions. Penta-cationic species are not well-described, but our data indicate that electrostatics are not the only determinant of drug localization; otherwise, both analogues would localize to the mitochondria, as has been reported for some monocations.[14] Membrane transport is described by a three-stage model that requires the molecule to initially adsorb onto the membrane, then translocate through the lipid bilayer, and finally desorb from the inner side of the membrane.[16] As the lipid boundaries of intracellular organelles vary markedly in composition, it is possible that localization is a function of the interactions between the Mn porphyrins and cellular membranes. Another possibility is that drug binding to intracellular targets determines cellular location. For MnTE-2-PyP^{5+} one potential target is DNA; however, the nonplanar ortho porphyrin isomers are weak DNA intercalators,[17] and the overlap between the P and Mn maps (Figure 3) is only partially coincident, data which do not support a strong DNA binding interaction but may indicate a weaker binding equilibrium.

To probe the implications of drug partitioning, we then examined the effects of drug distribution upon pharmacological activity. For these experiments, the cells were challenged with high concentrations of superoxide, generated via the agent menadione.[18] As menadione redox cycles in the mitochondria,[18] we hypothesized that if MnTnHex-2-PyP^{5+} was mitochondrial based, it would prove efficacious in converting the superoxide

dx.doi.org/10.1021/ic300700g | Inorg. Chem. 2013, 52, 4121−4123

flux into hydrogen peroxide, a more damaging ROS.[19] Hence, under these conditions, MnTnHex-2-PyP^{5+} should act as a superior pro-oxidant to MnTE-2-PyP^{5+} and augment menadione's toxicity.[19] This hypothesis was tested by poising the menadione concentration at the maximum noncytotoxic level and examining the combination effect (Figure 5). Both drugs

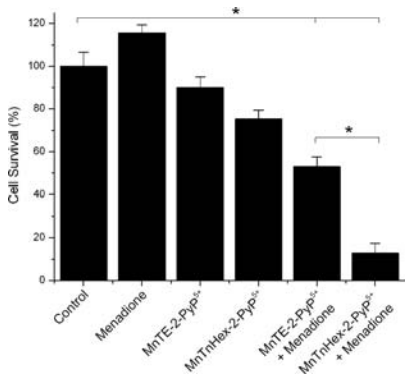

Figure 5. Intracellular drug distribution determines pharmacological activity. A549 cells were pretreated with drug (100 μM) for 24 h and then exposed to a nontoxic dose of menadione (10 μM) for a further 24 h.

caused a significant enhancement of menadione's toxicity, and in accord with our hypothesis, pretreating with MnTnHex-2-PyP^{5+} decreased cell survival 5-fold when compared to MnTE-2-PyP^{5+}.

Intracellular localization therefore has a significant effect upon drug action. This may explain the differences in both pro- and anti- oxidant efficacies when the two drugs are compared in disease models.[20] In particular, the nuclear localization of MnTE-2-PyP^{5+} may explain why this analogue, and not MnTnHex-2-PyP^{5+}, is able to prevent the formation of 8-OHdG, a biomarker of DNA damage.[21] Conversely our data shows that MnTnHex-2-PyP^{5+} is more effective at enhancing the pro-oxidant activity of mitocondrial ROS. Differences in localization may also contribute toward other drug properties. For example, the nuclear targeting of MnTE-2-PyP^{5+} may enhance its ability to oxidize transcription factors such as NF-κB, an event which is known to inhibit gene transcription.[22,23] Drug localization should therefore be included as a design criteria when developing this drug class, an advance which promises to provide more effective and selective therapeutics.

■ ASSOCIATED CONTENT

Ⓢ Supporting Information

Protocols and experimental detail for SRIXE data acquisition. This material is available free of charge via the Internet at http://pubs.acs.org.

■ AUTHOR INFORMATION

Corresponding Author

*E-mail gregory.giles@otago.ac.nz.

Notes

The authors declare no competing financial interest.

■ ACKNOWLEDGMENTS

This work was supported by Lottery Health and a University of Otago Research Grant (G.I.G.) and an ARC Discovery grant and Professorial Fellowship (P.A.L.). Use of the Advanced Photon Source was supported by the U.S. DOE under Contract No. DE-AC02-06CH11357. Travel was provided by the New Zealand Synchrotron Group and the Australian Synchrotron Research Program (ASRP). The ASRP was funded by the Commonwealth of Australia under the Major National Research Facilities Program.

■ ABBREVIATIONS

MnTE-2-PyP^{5+} [Mn(TE-2-PyP)]$^{5+}$, Mn(III) *meso*-tetrakis(*N*-ethylpyridinium-2-yl)porphyrin; MnTnHex-2-PyP^{5+} [Mn(TnHex-2-PyP)]$^{5+}$, Mn(III) *meso*-tetrakis(*N*-*n*-hexylpyridinium-2-yl)porphyrin

■ REFERENCES

(1) Reuter, S.; Gupta, S. C.; Chaturvedi, M. M.; Aggarwal, B. B. *Free Radical Biol. Med.* **2010**, *49*, 1603−1616.
(2) Batinic-Haberle, I.; Rajic, Z.; Tovmasyan, A.; Reboucas, J. S.; Ye, X.; Leong, K. W.; Dewhirst, M. W.; Vujaskovic, Z.; Benov, L.; Spasojevic, I. *Free Radical Biol. Med.* **2011**, *51*, 1035−1053.
(3) Batinic-Haberle, I.; Reboucas, J. S.; Spasojevic, I. *Antioxid. Redox Signaling* **2010**, *13*, 877−918.
(4) Halliwell, B. *Bull. Eur. Physiopathol. Respir.* **1981**, *Suppl 17*, 21−29.
(5) Beckman, J. S.; Beckman, T. W.; Chen, J.; Marshall, P. A.; Freeman, B. A. *Proc. Natl. Acad. Sc.i U.S.A.* **1990**, *87*, 1620−1624.
(6) Mao, G. D.; Thomas, P. D.; Lopaschuk, G. D.; Poznansky, M. J. *J. Biol. Chem.* **1993**, *268*, 416−420.
(7) Aitken, J. B.; Carter, E. A.; Eastgate, H.; Hackett, M. J.; Harris, H. H.; Levina, A.; Lee, Y. C.; Chen, C. I.; Lai, B.; Vogt, S.; Lay, P. A. *Radiat. Phys. Chem.* **2010**, *79*, 176−184.
(8) Batinic-Haberle, I.; Spasojevic, I.; Stevens, R. D.; Hambright, P.; Fridovich, I. *J. Chem. Soc., Dalton Trans.* **2002**, 2689−2696.
(9) Ferrer-Sueta, G.; Vitturi, D.; Batinic-Haberle, I.; Fridovich, I.; Goldstein, S.; Czapski, G.; Radi, R. *J. Biol. Chem.* **2003**, *278*, 27432−27438.
(10) Spasojevic, I.; Chen, Y.; Noel, T. J.; Fan, P.; Zhang, L.; Reboucas, J. S.; St Clair, D. K.; Batinic-Haberle, I. *Free Radical Biol. Med.* **2008**, *45*, 943−949.
(11) Aitken, J. B.; Lay, P. A.; Duong, T. T.; Aran, R.; Witting, P. K.; Harris, H. H.; Lai, B.; Vogt, S.; Giles, G. I. *J. Biol. Inorg. Chem.* **2012**, *17*, 589−598.
(12) Schwartz, J. L.; Tamura, Y.; Jordan, R.; Grierson, J. R.; Krohn, K. A. *J. Nucl. Med.* **2003**, *44*, 2027−2032.
(13) Dessolin, J.; Schuler, M.; Quinart, A.; De Giorgi, F.; Ghosez, L.; Ichas, F. *Eur. J. Pharmacol.* **2002**, *447*, 155−161.
(14) Ross, M. F.; Prime, T. A.; Abakumova, I.; James, A. M.; Porteous, C. M.; Smith, R. A.; Murphy, M. P. *Biochem. J.* **2008**, *411*, 633−645.
(15) Miriyala, S.; Spasojevic, I.; Tovmasyan, A.; Salvemini, D.; Vujaskovic, Z.; St Clair, D.; Batinic-Haberle, I. *Biochim. Biophys. Acta* **2012**, *1822*, 794−814.
(16) Cafiso, D. S.; Hubbell, W. L. *Annu. Rev. Biophys. Bioeng.* **1981**, *10*, 217−244.
(17) Spasojević, I.; Menzeleev, R.; White, P. S.; Fridovich, I. *Inorg. Chem.* **2002**, *41*, 5874−5881.
(18) Fukui, M.; Choi, H. J.; Zhu, B. T. *Toxicol. Appl. Pharmacol.* **2012**, *262*, 156−166.
(19) Ohsea, T.; Nagaoka, S.; Arakawa, Y.; Kawakami, H.; Nakamura, K. *J. Inorg. Biochem.* **2001**, *85*, 201−208.
(20) Pollard, J. M.; Reboucas, J. S.; Durazo, A.; Kos, I.; Fike, F.; Panni, M.; Gralla, E. B.; Valentine, J. S.; Batinic-Haberle, I.; Gatti, R. A. *Free Radical Biol. Med.* **2009**, *47*, 250−260.
(21) Gauter-Fleckenstein, B.; Fleckenstein, K.; Owzar, K.; Jiang, C.; Batinic-Haberle, I.; Vujaskovic, Z. *Free Radical Biol. Med.* **2008**, *44*, 982−989.
(22) Tse, H. M.; Milton, M. J.; Piganelli, J. D. *Free Radical Biol. Med.* **2004**, *36*, 233−247.
(23) Jaramillo, M. C.; Briehl, M. M.; Crapo, J. D.; Batinic-Haberle, I.; Tome, M. E. *Free Radical Biol. Med.* **2012**, *25*, 1272−1284.